Tensile and Impact Properties of Tungsten-Rhenium Alloy for Plasma-Facing Components in Fusion Reactor

Shotaro Watanabe[1], Shuhei Nogami[2], Jens Reiser[3], Michael Rieth[4], Sven Sickinger[5],

Siegfried Baumgärtner[6], Takeshi Miyazawa[7], Akira Hasegawa[8]

[1]   Department of Quantum Science and Energy Engineering, Graduate School of Engineering,
Tohoku University, 6-6-01-2, Aramaki-aza-Aoba, Aoba-ku, Sendai 980-8579, Japan,
shotaro.watanabe.s5@dc.tohoku.ac.jp

[2]   Department of Quantum Science and Energy Engineering, Graduate School of Engineering,
Tohoku University, 6-6-01-2, Aramaki-aza-Aoba, Aoba-ku, Sendai 980-8579, Japan,
shuhei.nogami@qse.tohoku.ac.jp

[3]   Institute for Applied Materials, Karlsruhe Institute of Technology, Hermann-von-
Helmholtz-Platz 1, 76344 Eggenstein-Leopoldshafen, Germany, jens.reiser@kit.edu

[4]   Institute for Applied Materials, Karlsruhe Institute of Technology, Hermann-von-
Helmholtz-Platz 1, 76344 Eggenstein-Leopoldshafen, Germany, michael.rieth@kit.edu

[5]   Institute for Applied Materials, Karlsruhe Institute of Technology, Hermann-von-
Helmholtz-Platz 1, 76344 Eggenstein-Leopoldshafen, Germany, sven.sickinger@kit.edu

[6]   Institute for Applied Materials, Karlsruhe Institute of Technology, Hermann-von-
Helmholtz-Platz 1, 76344 Eggenstein-Leopoldshafen, Germany,
siegfried.baumgaertner@kit.edu

[7]   Department of Quantum Science and Energy Engineering, Graduate School of Engineering,
Tohoku University, 6-6-01-2, Aramaki-aza-Aoba, Aoba-ku, Sendai 980-8579, Japan,
takeshi.miyazawa.c7@tohoku.ac.jp

[8] Department of Quantum Science and Energy Engineering, Graduate School of Engineering, Tohoku University, 6-6-01-2, Aramaki-aza-Aoba, Aoba-ku, Sendai 980-8579, Japan, akira.hasegawa@qse.tohoku.ac.jp

Corresponding Author

Name   Shuhei Nogami

Postal address   Department of Quantum Science and Energy Engineering, Graduate School

of Engineering, Tohoku University, 6-6-01-2, Aramaki-aza-Aoba, Aoba-ku,

Sendai 980-8579, Japan

Telephone   +81-22-795-7923

Fax number   +81-22-795-7924

E-mail address   shuhei.nogami@qse.tohoku.ac.jp

Tensile and Impact Properties of Tungsten-Rhenium Alloy for Plasma-Facing Components in Fusion Reactor

Shotaro Watanabe[1], Shuhei Nogami[1], Jens Reiser[2], Michael Rieth[2], Sven Sickinger[2], Siegfried Baumgärtner[2], Takeshi Miyaawa[1], Akira Hasegawa[1]

[1] Department of Quantum Science and Energy Engineering, Graduate School of Engineering, Tohoku University, 6-6-01-2, Aramaki-aza-Aoba, Aoba-ku, Sendai 980-8579, Japan

[2] Institute for Applied Materials, Karlsruhe Institute of Technology, Hermann-von-Helmholtz-Platz 1, 76344 Eggenstein-Leopoldshafen, Germany

Abstract

Low temperature brittleness and high ductile-to-brittle transition temperature (DBTT) are potential drawbacks related to the mechanical properties of tungsten (W) for divertor application in fusion reactors. In the present study, to improve the mechanical properties of W, rhenium (Re) addition has been applied as a solid solution alloying method. In this paper, the effects of Re addition on the tensile and Charpy impact properties of W thick plate fabricated by powder metallurgy and hot rolling were investigated, which has enough volume as the plasma facing material and the microstructural uniformity for mass-production. At the temperature below 1000 °C, the W-3%Re showed 5–30% higher strength, 10–35% higher total elongation, 100 °C lower DBTT, and 16% higher upper shelf energy than those of the pure W.

1. Introduction

Tungsten (W) is the most promising as plasma facing material of the fusion reactor divertors because of its high melting point, high thermal conductivity, low tritium retention, and low sputtering rate. However, there remain some drawbacks related to the mechanical properties of W materials, e.g., low temperature brittleness, recrystallization-induced embrittlement, and neutron-irradiation-induced embrittlement. Therefore, it is necessary to develop W materials which have low temperature ductility and low ductile-to-brittle transition temperature (DBTT), high recrystallization temperature, and high resistance to neutron irradiation.

Several methods to suppress brittleness and improve mechanical properties of W have been reported. As examples of these methods, grain refining [1], work hardening [2], dispersion strengthening [3, 4], and solid solution alloying [3, 5] have been used. Alloying by rhenium (Re) is one of the common methods as solid solution alloying of W materials. It is well known that substitutional solid solution elements in body-center-cubic (bcc) metals like Re in W could cause solid solution strengthening at high temperature and solid solution softening at low temperature. It was reported that the swaged rods with 6 mm diameter made of W-1%Re, W-2%Re, W-7%Re, and W-25%Re showed higher ductility at low temperature and higher strength at high temperature than those of pure W rod with the same diameter as the W-Re alloys [6]. Also in the case of W-6%Re and W-8%Re swaged rods with 8 mm diameter, lower hardness at low temperature than that of pure W rod with the same diameter as the W-Re alloy was observed [7]. Moreover, forged rods made of W-5%Re and W-10%Re had higher fracture toughness at elevated temperature than pure W [8].

Solid solute Re in W materials could improve not only mechanical properties as mentioned before, but also resistance to recrystallization and neutron irradiation [9, 10]. Changes in the mechanical properties, resistance to recrystallization, and resistance to neutron

irradiation by Re addition are dependent on the additive amount of Re, which were schematically summarized by Fukuda et al. [11]. Strength and recrystallization temperature of pure W increased with additive amount of Re. However, the effects of Re on these properties were saturated with around 5% Re addition. The effect of Re addition on DBTT was different between as-worked and recrystallized materials. In the case of as-worked W-Re alloys, the more additive amount of Re made the DBTT lower, while the DBTT of recrystallized W-Re alloys was the lowest when the additive amount of Re was approximately 1–4% and 25%, which is similar to the solid solubility limit of Re in W [12]. Thermal conductivity of W decreased with increase in the additive amount of Re, which is one of the most important properties of the plasma facing material of divertors [13]. Furthermore, the approximately 3–10% additive Re was the most effective to suppress the irradiation hardening [14].

Most of the previous studies on the effects of Re on physical and thermo-mechanical properties of W materials before and after the neutron irradiation were performed using wires, small-diameter rods, and sheets made of W-Re alloys [6–8, 12], that would not be available as the plasma facing material of fusion reactor divertors. Thus, the objective of the present study is to evaluate the mechanical properties of W-Re alloy thick plate fabricated by a powder metallurgy, which has enough volume as the plasma facing material and the microstructural uniformity for mass-production and to discuss the effect of solute Re on grain structure, strength, ductility, and impact properties of the W thick plate.

2. Materials and Methods

The materials used in the present study were pure W and W-3%Re plate with a thickness of 7 mm, fabricated by powder metallurgy (cold isostatic pressing at room temperature and sintering at 1800–2200 °C) and hot rolling at 1400–1600 °C followed by a final heat treatment at approximately 900 °C for stress relief. The additive amount of Re (3%)

in the present study was determined based on the knowledge as mentioned in the last section. The reduction ratio (deformation ratio) for the hot rolling of these two plates were the same. Both materials were prepared in the as-received (hot-rolled and stress-relieved) condition.

To observe the grain structure and measure the grain size, mechanical polishing and electrolytic polishing using a solution of sodium hydroxide and potassium ferricyanide were conducted on the "L × T," "T × S," and "S × L" surfaces. The orientations of the L, T, and S directions are shown in Fig. 1. The L, T, and S directions is the rolling direction of the plate, is normal to the rolling direction, and is perpendicular to both L and T directions, respectively. The grain sizes were measured based on the ASTM E112-85 standard with metallographic optical microscope images after polishing [15].

To investigate the tensile properties (ultimate tensile strength (UTS), 0.2% proof stress ($\sigma_{0.2}$), uniform elongation (UE), total elongation (TE), and reduction in area (RA)) of the pure W and W-3%Re, tensile tests were carried out at temperatures ranging from room temperature to 1300 °C in vacuum at a strain rate of 1×10^{-3} s^{-1}. An SS-J type tensile specimen was used, which has 5 mm gauge length, 1.2 mm gauge width, and 0.5 mm thickness. The loading axis of the specimens was aligned along the L direction (rolling direction) of the materials. Fractured specimens by the tensile tests were observed using a scanning electron microscope (SEM) to measure the RA and to clarify the fracture manner.

To investigate the Charpy impact properties of the pure W and W-3%Re, Charpy impact tests were performed based on the EU standard DIN EN ISO 14556:2017-05 [16]. Charpy impact tests were carried out using a KLST-type Charpy V-notched specimens (27 mm length, 3 mm width, 4 mm height, 1 mm notch depth, 0.1mm notch root radius, and 22 mm span) along L-S direction (see Fig. 1) using a testing machine installed at Karlsruhe Institute of Technology at temperatures ranging from 400 °C to 1000 °C in vacuum. The first letter (L) indicates the direction perpendicular to the expected crack plane while the second letter (S)

stands for the expected direction of crack growth. To clarify the fracture manner of the pure W and W-3%Re, the fracture surfaces close to the V-notch of the specimens after Charpy impact test were observed using an SEM.

3. Results

3.1 Grain structure

The optical microscope images of grain structure of the as-received pure W and W-3%Re are shown in Fig. 2 [17]. Flattened grain structures elongated along rolling direction like "pancake" were observed in two materials. Such grain structures were characteristic for W plates fabricated by powder sintering and hot rolling [18]. Fig. 3 shows the average grain sizes along L direction (d_L), T direction (d_T), and S direction (d_S) of the as-received pure W and W-3%Re measured using optical microscope images shown in Fig. 2 [17]. The d_L, d_T, and d_S of the as-received pure W and W-3%Re were 98 and 52 μm, 59 and 32 μm, and 22 and 19 μm, respectively.

3.2 Tensile properties

Figs. 4 (a) and (b) show the test temperature dependence of UTS and $\sigma_{0.2}$ of the as-received pure W and W-3%Re obtained by the tensile tests along L direction, respectively [19, 20]. The UTS and $\sigma_{0.2}$ of both materials decreased with increase in the test temperature. At the test temperature below 1300°C, the W-3%Re showed higher UTS and $\sigma_{0.2}$ than those of the pure W. The strength of W-3%Re was 5–30% higher below 1000 °C and 3–8 times higher at 1300°C. At room temperature and 100 °C, no $\sigma_{0.2}$ of the pure W was observed because of the fracture within an elastic deformation region. At 1300 °C, the UTS and $\sigma_{0.2}$ of pure W showed significant reduction compared to the W-3%Re.

Figs. 4 (c), (d), and (e) show the test temperature dependence of UE, TE, and RA of

the as-received pure W and W-3%Re obtained by the tensile tests along L direction, respectively [19, 20]. The RA was measured using SEM images of specimens after tensile test. At the test temperature below 200–300 °C, the UE, TE, and RA of the pure W and W-3%Re increased with test temperature. At temperatures ranging from 200–300 °C to 700–900 °C, the UE and TE of both materials decreased with increase in the test temperature, while the RA increased. At temperatures ranging from 700–900 °C to 1300 °C, changes of the UE and TE of W-3%Re by increase in the test temperature was small, while those of the pure W significantly increased. The RA of both materials increased with the test temperature at this temperature range and grew up to 100% at 1300 °C. At temperatures below 700–900 °C, the W-3%Re showed 2–6 times higher UE and 10–35% higher TE compared to the pure W, while the UE and TE of pure W were 3–30 times higher than those of W-3%Re at 1300 °C. In contrary, the RA of W-3%Re was lower than that of the pure W at all temperatures below 1300 °C. Although the pure W showed no elongation at room temperature and 100 °C, the W-3%Re showed UE and TE above zero (approximately 0.3% of UE) even at room temperature.

SEM images of the fracture surface of the pure W and W-3%Re after tensile tests at 100, 200, 600 and 1300 °C are shown in Fig. 5. At the test temperature below 200 °C, both pure W and W-3%Re showed a cleavage fracture surface (see Figs. 5 (a), (b), (e), and (f)). At temperatures ranging from 300 to 900 °C, a ductile fracture with delamination in the L × T planes was observed on the fracture surfaces of both materials (see Figs. 5 (c) and (g)). At 1300 °C, dimples were formed in the fracture surfaces of both pure W and W-3%Re (see Figs. 5 (d) and (h)). At all temperatures below 1300 °C, no significant differences between pure W and W-3%Re in the fracture manner at the same test temperature were observed although the test temperature dependences of the strength and ductility were different between them.

3.3 Charpy impact properties

Fig. 6 shows the test temperature dependence of absorbed energy of the as-received pure W and W-3%Re obtained by the Charpy impact tests along L-S direction [17]. Fig. 7 shows the appearances of specimens after the Charpy impact test. At 400 °C, the specimens made of both pure W and W-3%Re broke into two parts and showed a brittle fracture with no deformation and lateral expansion. The absorbed energies of both materials at this temperature were close to zero. At 500 °C, a mixture of brittle and delamination fractures was observed for the pure W, while the W-3%Re showed just a delamination fracture. The direction of delamination was parallel to the rolling direction (L direction) for both materials. The absorbed energies of the pure W and W-3%Re at this temperature were close to zero and 6.4 J, respectively. At the test temperature above 600 °C, both materials showed a delamination fracture accompanied by relatively high absorbed energies. A clear difference in the DBTT and upper shelf energy (USE) between two materials was observed, which was the average values of the absorbed energy from the DBTT to 1100 °C. The DBTTs and USEs of the pure W and W-3%Re were approximately 550 °C and 5.5 J and 450 °C and 6.4 J, respectively. Approximately 100 °C reduction in the DBTT and 20% increase in the USE were caused by the Re addition.

Fig. 8 shows the SEM images of fracture surfaces of the as-received pure W and W-3%Re after Charpy impact test at 400, 600, 800, and 900 °C [20]. Below the DBTT, a clear difference in the fracture manner between two materials was observed. The pure W showed a cleavage fracture at 400 °C, while the W-3%Re showed an intergranular fracture at sub-grain boundaries, as shown in Figs. 8 (a) and (d). According to the report by Curry and Knott [21], the cleavage fracture stress of several steels could increase with refining the grain size. Therefore, cleavage fracture was suppressed in the W-3%Re because of grain refining compared to the pure W. On the other hand, no difference in the fracture manner between two materials was observed above the DBTT. As shown in Figs. 8 (b), (c), (e), and (f), the fracture

10

surfaces showed intergranular at sub-grain boundaries, which were observed in both materials at all test temperatures above the DBTT and below 1000 °C. The size of sub-grain was approximately 3 μm regardless of materials and test temperature.

4. Discussion

The W-3%Re showed smaller grain than those of the pure W regardless of the direction (d_L, d_T, and d_S), as shown in Fig. 3. Effects of temperature and reduction ratio (deformation ratio) during hot-rolling could be negligible because these values were the same for two materials. Thus, it is assumed that W-3%Re produced finer grain structure compared to the pure W because the migration of grain boundaries accompanied by recrystallization during hot-rolling were inhibited by solute Re [22].

As mentioned in the chapter 3.2, the W-3%Re showed higher strength below 1300 °C, which could be attributed to the solid solution strengthening effect caused by the substitutional solid solute Re, as mentioned in the section 1. In addition to the solid solution strengthening, the grain refining could also lead to strengthening, which can be explained in general by the Hall–Petch law [23, 24]. Improvement in the mechanical properties by grain refining have been observed for most metals including W [25, 26]. Especially at 1300 °C, the strength of pure W rapidly decreased compared to the W-3%Re. This rapid reduction with increase in the test temperature could be induced by the recrystallization, as mentioned later.

W-3%Re showed higher elongation except at 1300 °C, which could be attributed to the solid solution softening effect caused by the substitutional solid solute Re, as mentioned in the section 1. Especially, it was remarkable that the UE and TE of W-3%Re were above zero at room temperature and 100 °C although the pure W showed no elongation. At 1300 °C, the elongation of pure W rapidly increased, while that of W-3%Re showed relatively small change

with increase in the test temperature. This rapid increase could be induced by the recrystallization, as mentioned later.

In general, the material showing higher strain hardening could produce lower RA, which is quantitatively described by the work hardening coefficient. In addition, the material with higher work hardening coefficient could produce higher UE [27]. Thus, the lower RA of W-3%Re compared to pure W could be explained by the increase in the work hardening coefficient accompanied by the increase in UE. Quantitative evaluations of the Re effect on the work hardening coefficient, RA, and UE are planned as future work.

As mentioned before, the strength and elongation of pure W rapidly decreased and increased at 1300 °C compared to the W-3%Re, respectively. It is well known that the recrystallized W materials show lower strength and higher elongation compared to the worked and stress-relieved W materials [8, 28]. The dislocation density in recrystallized grains is very low in general and the lack of dislocation could induce the strength reduction and elongation increase. Fig. 9 shows the optical micrographs of L × S surface of pure W and W-3%Re in the as-received condition and in the condition after annealing at 1300 °C for 1 h. After the annealing at 1300 °C, the pure W showed disappearance of flattened grain structures elongated along L direction and recrystallized grains accompanied by the grain growth. In contrary, the flattened grain structures elongated along L direction of the W-3%Re were maintained after the annealing. Thus, no recrystallization occurred in the W-3%Re after the annealing at 1300 °C for 1 h because the migration of grain boundaries was inhibited by solute Re [22]. Therefore, rapid decrease in the strength and increase in the elongation of pure W at 1300 °C could be caused by the recrystallization, which was not occurred in the W-3%Re.

It is known that the DBTT of materials with flattened grain structures elongated along L direction (rolling direction), which shows a delamination fracture on the L × T surface, decreases with grain refining along S direction [29]. In our previous study [17], it was clarified

that both DBTT and USE of pure W materials by powder metallurgy from different production routes could be determined by the grain size along the thickness (d_S), and the following Hall–Petch-type relation could be applied [23, 24, 30, 31]:

$$DBTT = A_{DBTT} - K_{DBTT} \cdot d_S^{-1/2} \qquad (1)$$

$$USE = A_{USE} - K_{USE} \cdot d_S^{-1/2} \qquad (2)$$

where A_{DBTT} [°C], A_{USE} [J], K_{USE} [J·μm$^{1/2}$], and K_{DBTT} [°C·μm$^{1/2}$] were constants independent of the grain size. These relations indicated that grain refining along S direction could cause a decrease in the DBTT and an increase in the USE of W materials. In the present study, to evaluate the effect of grain refining on the Charpy impact properties of the W-Re alloy and to discuss the effects of solid solute Re on the impact properties of W materials, Eqs. (1) and (2) were applied to the W-3%Re. Figs. 10 (a) and (b) show the relationships between the grain size along the thickness (d_S) and the DBTT and USE obtained by Charpy impact tests along L-S direction of the pure W and W-3%Re in the present study, the pure W plate with a thickness of 4 mm, and the pure W round-blank with a thickness of 29 mm by the previous studies [17, 32, 33]. The values of d_S, DBTT, and USE of 4 mm thick plate and 29 mm thick round blank were 19 μm, 450 °C, and 6.8 J and 63 μm, 710 °C, and 4.0 J, respectively. The USEs were the average values of the absorbed energy above the DBTT to 1000 °C. The error bars indicate the difference of the maximum and minimum absorbed energies from the USE. As shown in Figs. 10 (a) and (b), Eqs. (1) and (2) fit the experimentally determined DBTT and USE of pure W materials by powder metallurgy from different production routes very well, while the DBTT and USE of W-3%Re were slightly lower and higher than those expected by the Eqs. (1) and (2). The Hall–Petch-type relations include only the factor of grains. On the other hand, the effect of Re addition roughly consists of the effects of grain refining caused by the inhibition

13

of the grain boundary migration by the solute Re and the effects of solid solution strengthening and softening caused by the solute Re. Therefore, the improvement of Charpy impact properties of W due to the Re addition in the present study could be attributed to both grain refining and solid solution strengthening/softening.

To discuss the effects of the strength and ductility on the Charpy impact properties at test temperatures above the DBTT, the correlation between the absorbed energy from the Charpy impact tests described in section 3.3 and the tensile properties described in section 3.2 was evaluated. Fig. 11 shows the relationships between the Charpy absorbed energy above the DBTT and the tensile properties (UTS, $\sigma_{0.2}$, UE, TE, and RA) at the same test temperature for the pure W and W-3%Re in the present study and the pure W plate with a thickness of 4 mm by the previous study [17]. The test results at temperatures below the DBTT, where brittle fracture with a very low or zero absorbed energy was detected from the Charpy impact tests, are not included in this figure. As shown in Figs. 11 (a) and (b), the Charpy absorbed energy above the DBTT increased with the UTS and $\sigma_{0.2}$. In contrast, no clear correlations between the Charpy absorbed energy and the UE, TE, and RA were observed, as shown in Figs. 11 (c), (d), and (e). Therefore, it was possible that a material's strength could directly affect the Charpy absorbed energy above the DBTT. On the other hand, it was not certain whether the elongations and reduction in area, which were factors that determine a material's ductility, could directly affect the Charpy absorbed energy.

As a last discussion topic, effect of the Re produced by solid transmutation under the neutron irradiation environment of fusion reactor should be pointed out. All Re atoms in the W-3%Re of the present study was in the solid solute condition. In contrast, the W-Re precipitates and Re-enriched clusters could be produced by the transmutation [34]. As shown in the present study, the solid solute Re could induce a lot of positive effects. However, significant irradiation hardening could be caused by the W-Re precipitates and Re-enriched

clusters [34, 35]. According to the report by Krautwasser *et al*. [36], the DBTT of W-10%Re grew higher than that of pure W by neutron irradiation with increase in the neutron dose, although that was lower than pure W before irradiation. Solid transmutation of Re could be unavoidable under the neutron irradiation environment of fusion reactor. Therefore, the change of mechanical properties of W caused by the solid transmutation should be considered to realize structural reliability under the long-term operation of fusion reactors.

5. Conclusion

The mechanical properties of W-3%Re thick plate fabricated by powder metallurgy and hot-rolling, which was developed for the plasma facing material of fusion reactor divertors, were investigated, and the effect of solute Re on the grain structure, strength, ductility, and Charpy impact properties of the W thick plate were discussed. The results of this study were summarized as follows:

(1) The improvement of tensile and Charpy impact properties and the suppression of recrystallization were observed as positive effects of 3% Re addition.

(2) The grain size of W-3%Re was 10–50% smaller than that of pure W.

(3) At the temperature below 1000 °C, the W-3%Re showed 5–30% higher strength, 2–6 times higher uniform elongation, and 10–35% higher total elongation than those of the pure W. The improvement of these properties by 3% Re addition could be caused by the grain refining effect and the effects of solid solution strengthening and softening.

(4) The strength and elongation of pure W rapidly decreased and increased at 1300 °C compared to the W-3%Re, respectively. It was clarified that recrystallization in the pure W and no recrystallization in the W-3%Re at 1300 °C could cause these differences.

(5) The improvement of Charpy impact properties of W due to 3% Re addition was observed,

which could be attributed to both grain refining and solid solution strengthening/softening. The DBTTs and USEs of the pure W and W-3%Re were 550 °C and 5.5 J and 450 °C and 6.4 J, respectively.

(6) It was expected that the suppression of the low temperature brittleness, lowering the DBTT, and the suppression of recrystallization, which were issues related to the thermo-mechanical properties of W materials for divertor application in fusion reactors, could be simultaneously improved by the Re addition.

Acknowledgement

References

[1] U. K. Vashi, R. W. Armstrong, G. E. Zima, Metall. Trans. **1** (1970) 1769–1771.

[2] Q. Wei and L. J. Kecskes, Mater. Sci. Eng. A **491** (2008) 62–69.

[3] P. Makarov, K. Povarova, Int. J. Ref. Met. and Hard Mater. **20** (2002) 277–285.

[4] P. Schade, Int. J. Ref. Met. and Hard Mater. **28** (2010) 648–660.

[5] A. Luo, K. S. Shin, D. L. Jacobson, Scr. Metall. **25** (1991) 2411–2414.

[6] P. L. Raffo, J. Less-common Met. **17** (1996) 133–149.

[7] J. E. Stephens, W. R. Witzke, J. Less-common Met. **23** (1971) 325–342.

[8] Y. Mutoh, K. Ichikawa, K. Nagata, M. Takeuchi, J. Mater. Sci. **30** (1995) 770–775.

[9] K. Tsuchida, T. Miyazawa, A. Hasegawa, S. Nogami, M. Fukuda, Nucl. Mater. Eng. **15** (2018) 158–163.

[10] M. Fukuda, T. Tanno, S. Nogami, A. Hasegawa, Mater. Trans. **53** (2012) 2145–2150.

[11] M. Fukuda, S. Nogami, A. Hasegawa, H. Usami, K. Yabuuchi, T. Muroga, Fus. Eng. Des. **89** (2014) 1033–1036.

[12] W. D. Klopp, J. Less-common Met. **43** (1975) 261-278.

[13] T. Tanabe, C. Eamchotchawalit, C. Busabok, S. Taweethavorn, M. Fujitsuka, T. Shikama, Mater. Let. **57** (2003) 2950–2953.

[14] T. Tannno, A. Hasegawa, J. C. He, M. Fujiwara, S. Nogami, M. Satou, T. Shishido, K. Abe, Mater. Trans. **48** (2007) 2399–2402.

[15] ASTM E112–85, Standard Methods for Determining the Average Grain Size, Annual Book of ASTM, 1986, 227–290.

[16] DIN EN ISO 14556:2017-05, Metallische Werkstoffe - Kerbschlagbiegeversuch nach Charpy (V-Kerb) - Instrumentiertes Prüfverfahren (ISO 14556:2015); Deutsche Fassung EN ISO 14556:2015 [in German].

[17] S. Nogami, S. Watanabe, J. Reiser, M. Rieth, S. Sickinger, A. Hasegawa, Fus. Eng. Des.

135 (2018) 196–203.

[18] M. Rieth, A. Hoffmann, Int. J. Refract. Met. Hard. Mater. **28** (2010) 679–686.

[19] M. Fukuda, S. Nogami, K. Yabuuchi, A. Hasegawa, T. Muroga, Fus. Sci. Technol. **68** (2015) 690–693.

[20] S. Nogami, S. Watanabe, J. Reiser, M. Rieth, S. Sickinger, A. Hasegawa, Fus. Eng. Des. **140** (2019) 48–61.

[21] D. A. Curry and J. F. Knott, Met. Sci. **12** (1978) 511–514.

[22] E. M. Savitskii, M. A. Tylkina, S. I. Ipatova, E. I. Pavlova, Met. Sci. Heat Treat. **2** (9) (1960) 483–486.

[23] E. O. Hall, Proc. Phys. Soc. London Sect. B **64** (1951) 747–753.

[24] N. J. Petch, J. Iron Steel Inst. London **173** (1953) 25–28.

[25] K. Farrell, A. C. Schaffhauser, J. O. Stiegler, J. Less-Common Met. **13** (1967) 141–155.

[26] C. Bonnekoh, A. Hoffmann, J. Reiser, Int. J. Refract. Met. Hard Mater. **71** (2018) 181–189.

[27] N. Tsuchida, T. Inoue, K. Enami, Mater. Trans. **53** (2012) 133–139.

[28] B. Gludovatz, S. Wurster, A. Hoffmann, R. Pippan, Int. J. Refract. Met. Hard Mater. **28** (2010) 674–678.

[29] Y. Kimura, T. Inoue, F. Yin, K. Tsuzaki, ISIJ Int. **50** (2010) 152–161.

[30] A. N. Stroh, Adv. Phys. **6** (1957) 48.

[31] T. Hanamura, F. Yin, K. Nagai, ISIJ Int. **44** (2004) 610–617.

[32] M. Rieth, D. Armstrong, B. Dafferner, S. Heger, A. Hoffmann, M.-D. Hoffmann, U. Jäntsch, C. Kübel, E. Materna-Morris, J. Reiser, M. Rohde, T. Scherer, V. Widak, H. Zimmermann, Adv. Sci. Technol. **73** (2010) 11–21.

[33] M. Rieth, J. Reiser, B. Dafferner, S. Baumgärtner, Fus. Sci. Technol. **61** (2012) 381–384.

[34] T. Hwang, A. Hasegawa, K. Tomura, N. Ebisawa, T. Toyama, Y. Nagai, M. Fukuda, T.

Miyazawa, T. Tanaka, S. Nogami, J. Nucl. Mater. **507** (2018) 78–86.

[35] M. Fukuda, N. A. P. Kiran Kumar, T. Koyanagi, L. M. Garrison, L. L. Snead, Y. Katoh, A. Hasegawa, J. Nucl. Mater. **479** (2016) 249–254.

[36] P. Krautwasser, H. Derz, E. Kny, Proc. 12th Int. Plansee Seminar, **1** (1989) 673–681.

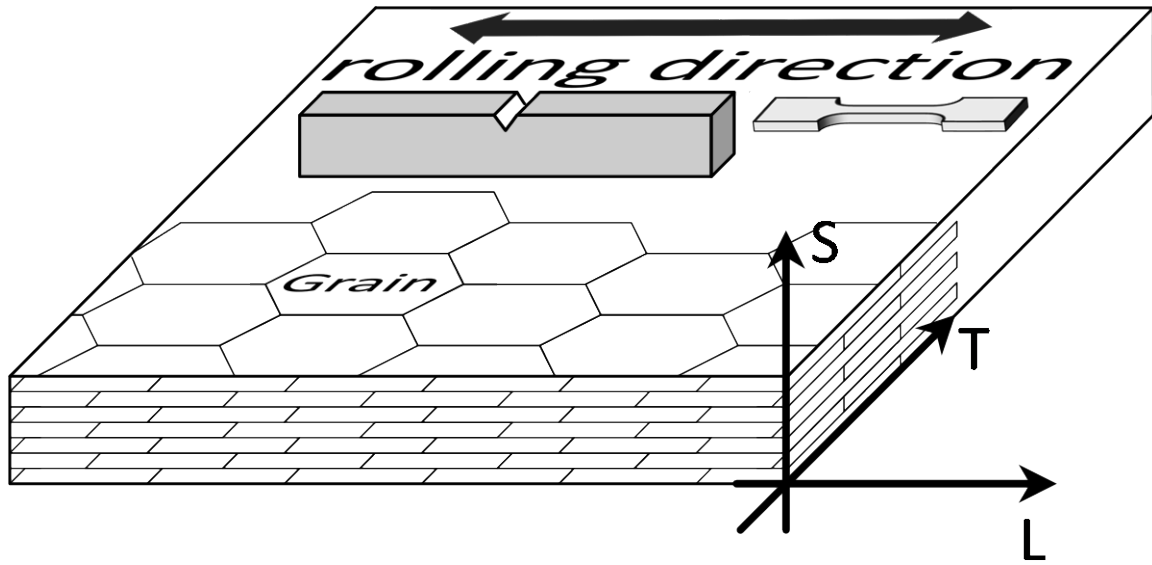Fig. 1 Nomenclature of directions of materials and specimens of tensile and Charpy impact tests.

Fig. 2 3D images of grain structure after electrolytic polishing obtained by optical microscope of as-received (a) pure W and (b) W-3%Re hot-rolled plates [17].

(a) Pure W   (b) W-3%Re

S.D.

T.D.

L.D.
(R.D.)
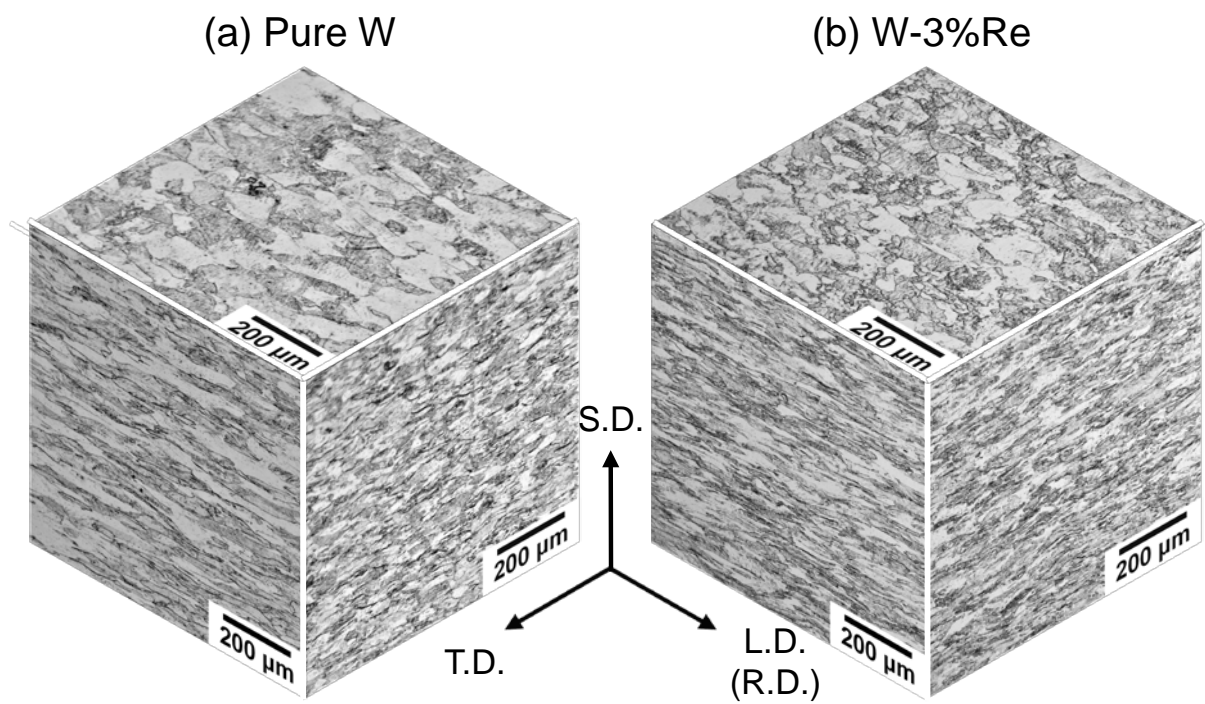
Fig. 3 Average grain sizes along L, T, and S directions (d_L, d_T, and d_S) of as-received pure W
and W-3%Re hot-rolled plates [17].
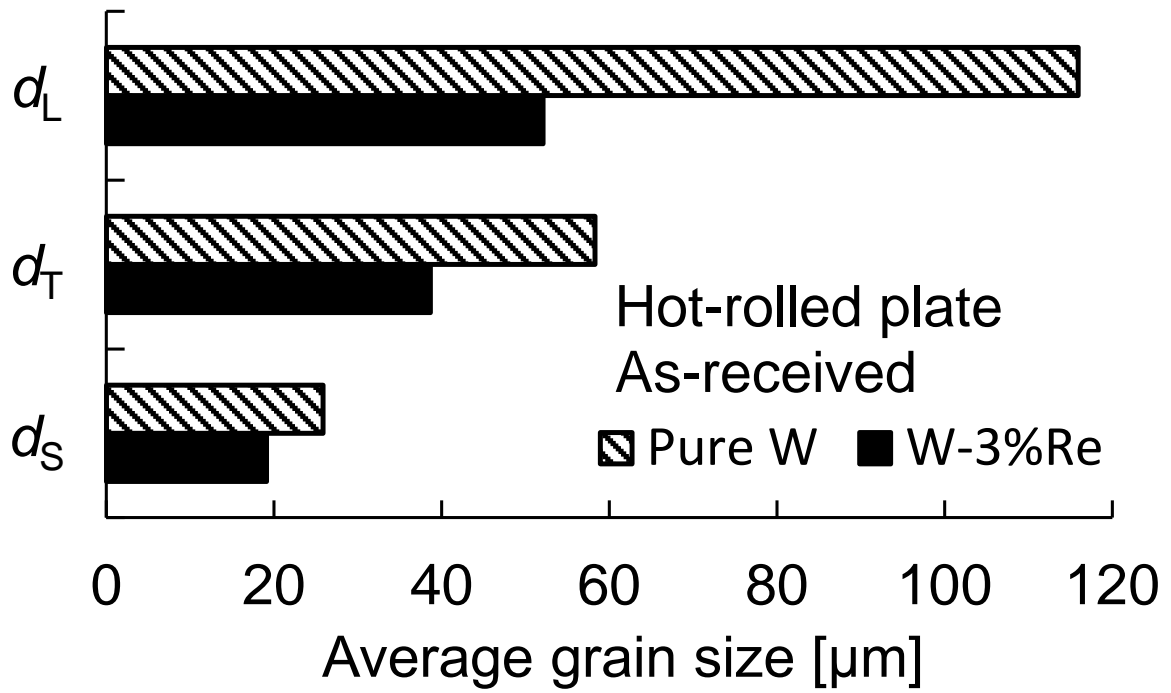
Fig. 4 Test temperature dependences of (a) ultimate tensile strength, (b) 0.2% proof stress, (c) uniform elongation, (d) total elongation, and (e) reduction in area by tensile tests (strain rate = 1×10^{-3} s^{-1}) using SS-J specimens along L direction of as-received pure W and W-3%Re hot-rolled plates [19, 20].
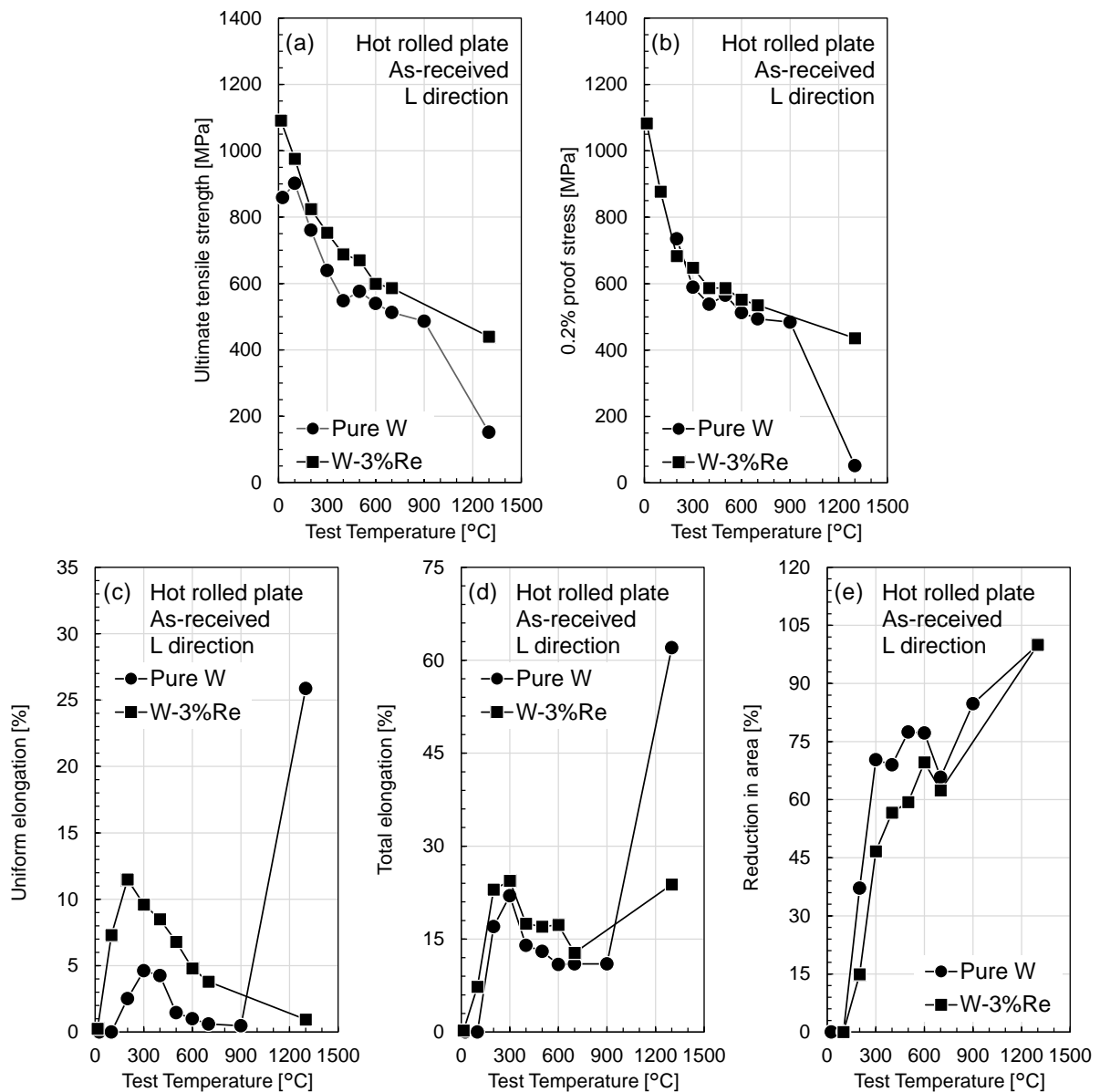
Fig. 5 Fracture surfaces obtained by SEM of specimens after tensile tests along L direction of as-received pure W and W-3%Re hot-rolled plates. Test temperature is (a, e) 100 °C, (b, f) 200 °C, (c, g) 600 °C, and (d, h) 1300 °C. The values of reduction in area (RA) are shown at the upper right in each SEM image.
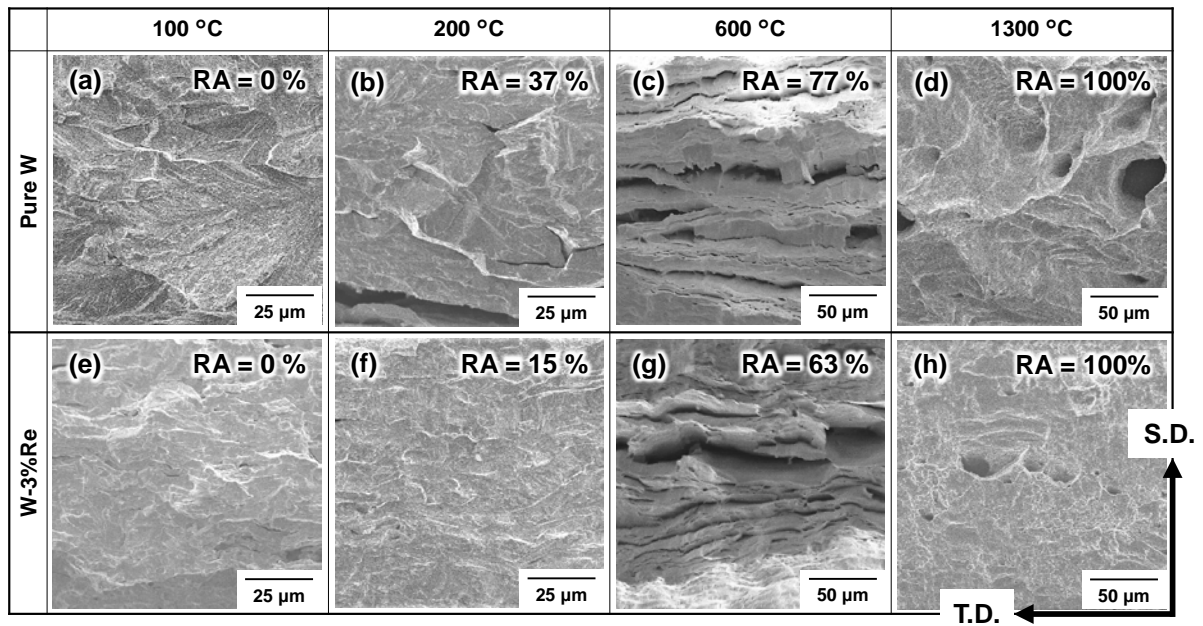
Fig. 6 Test temperature dependences of absorbed energy from Charpy impact tests of KLST specimens (L-S direction) of as-received pure W and W-3%Re hot-rolled plates [17].
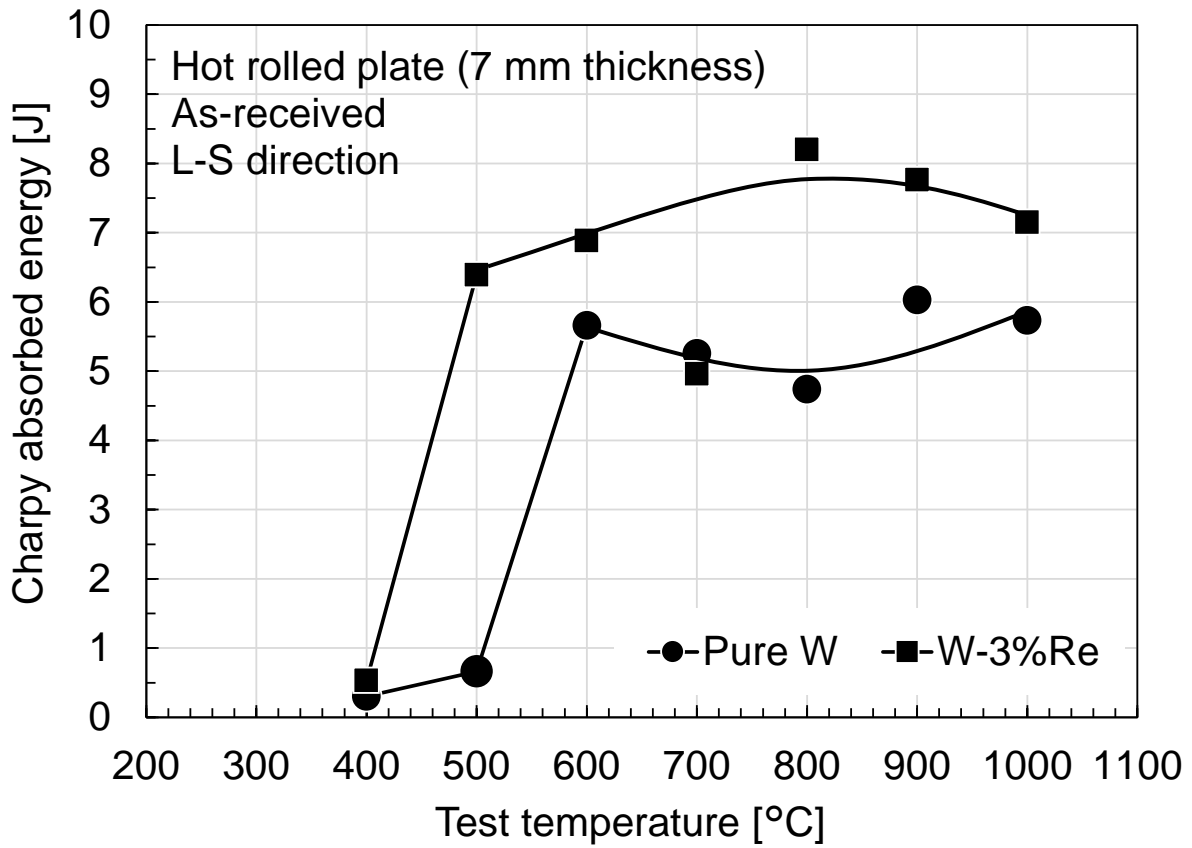
Fig. 7 Appearances of KLST specimens after Charpy impact tests (L-S direction) of as-received (a) pure W and (b) W-3%Re hot-rolled plates [17]. Descriptions in the right column for each specimen indicate fracture manner.

(a) Pure W		(b) W-3%Re	
1000 °C	Delamination	1000 °C	Delamination
900 °C	Delamination	900 °C	Delamination
800 °C	Delamination	800 °C	Delamination
700 °C	Delamination	700 °C	Delamination
600 °C	Delamination	600 °C	Delamination
500 °C	Brittle + Delamination	500 °C	Delamination
400 °C	Brittle	400 °C	Brittle + Delamination

Fig. 8 Fracture surfaces obtained by SEM of specimens after Charpy impact tests (L-S direction) of as-received pure W and W-3%Re hot-rolled plates tested at (a, d) 400 °C, (b, e) 600 °C, (c) 900, and (f) 800 °C [20].
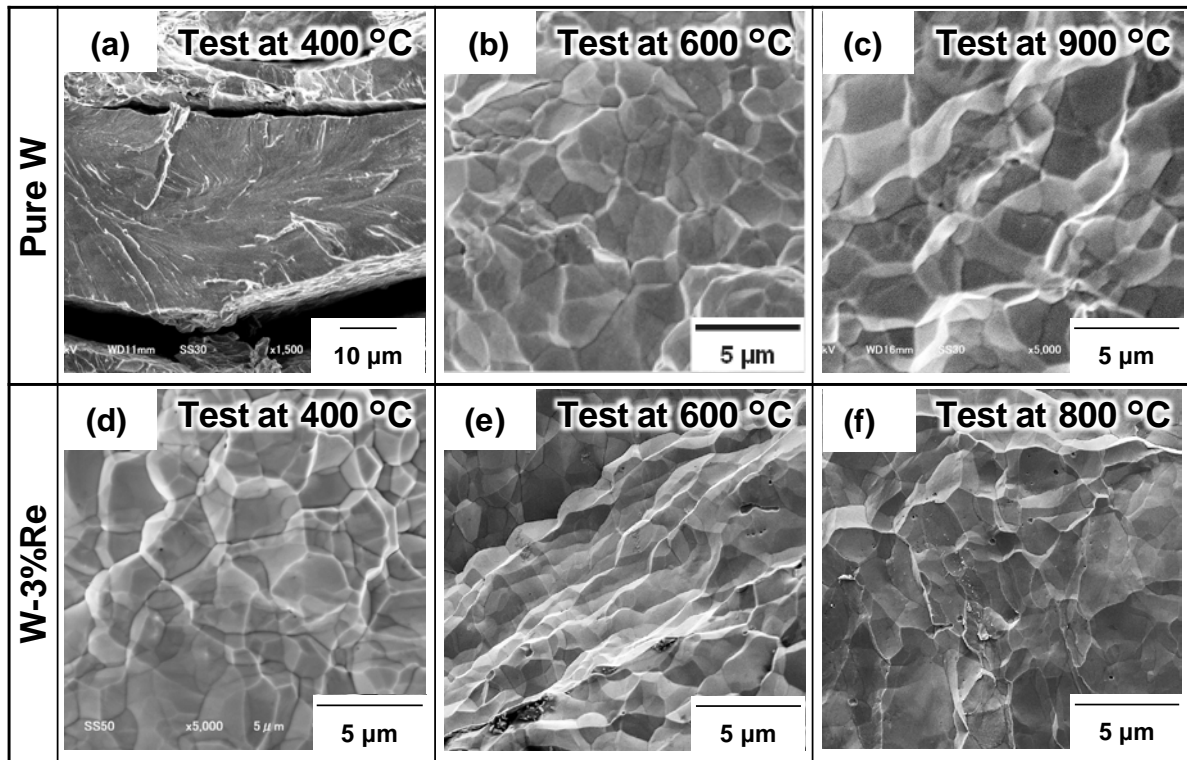
Fig. 9 2D images of grain structure after electrolytic polishing obtained by optical microscope of L × S surface of pure W and W-3%Re hot-rolled plates in (a) as-received condition and (b) condition after annealing at 1300 °C for 1 h.
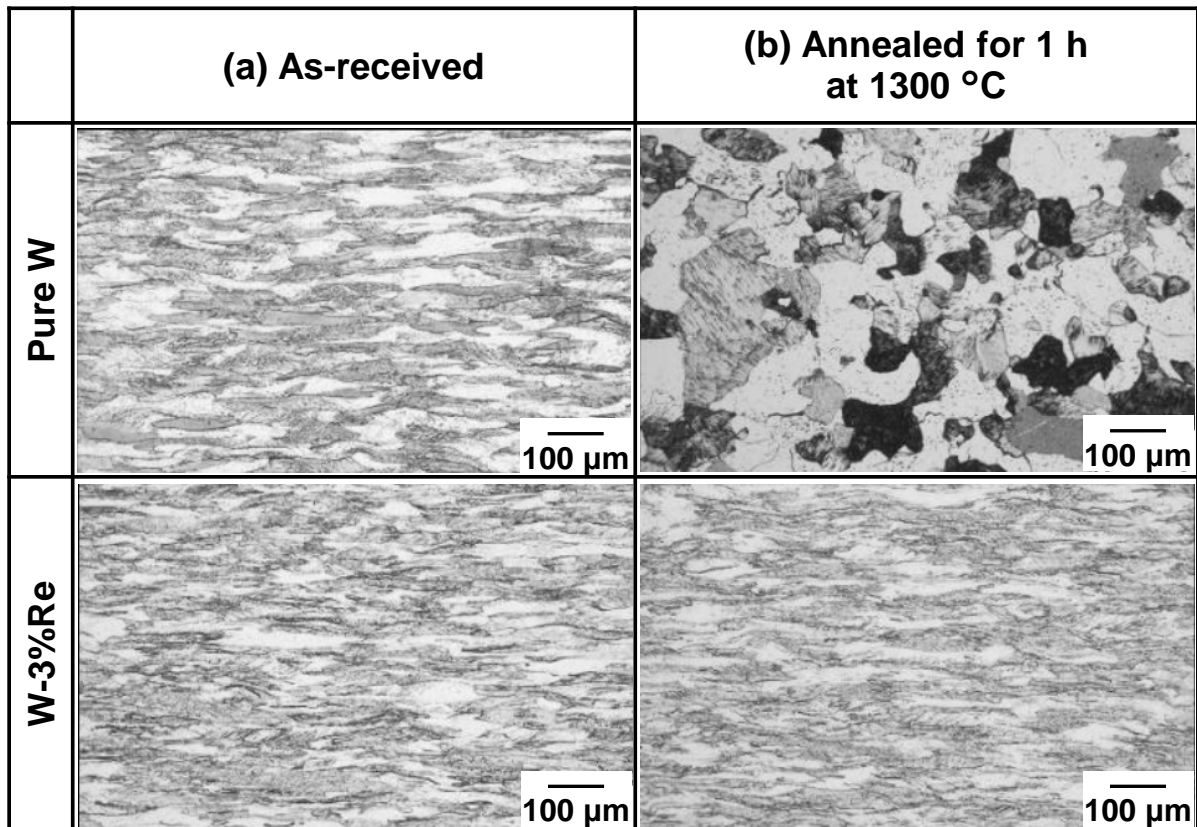

	(a) As-received	(b) Annealed for 1 h at 1300 °C
Pure W	100 µm	100 µm
W-3%Re	100 µm	100 µm

Fig. 10 Relationships between grain size along thickness (d_S) and (a) DBTT and (b) USE obtained by Charpy impact tests of KLST specimens (L-S direction) of the as-received pure W and W-3%Re hot-rolled plates in the present study, the as-received pure W hot-rolled plate with a thickness of 4 mm, and the as-received pure W round-blank with a thickness of 29 mm [17, 32, 33]. The USEs are the average values of absorbed energy above DBTT and below 1000 °C.
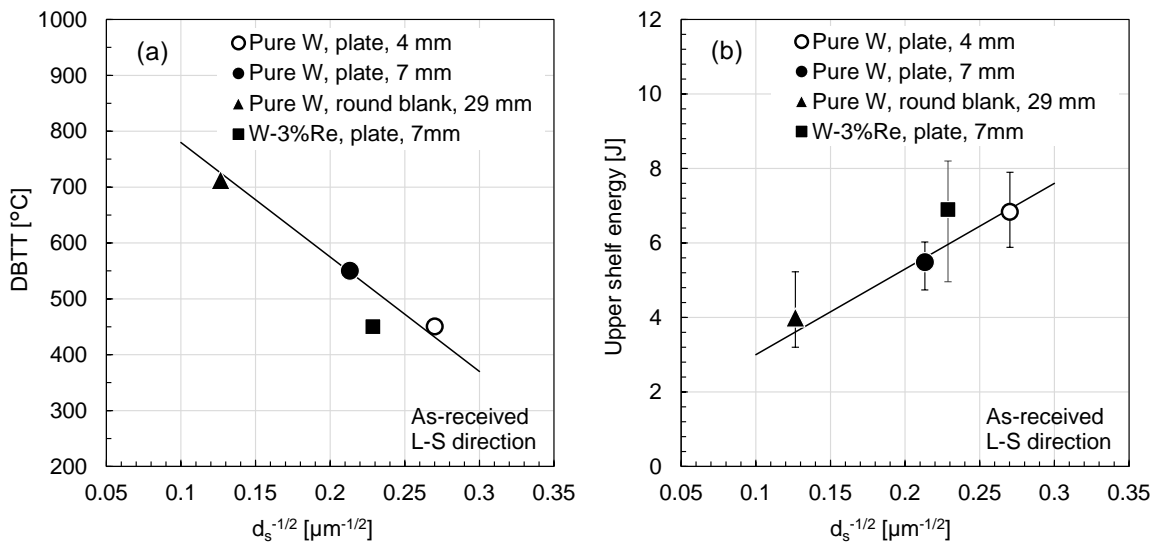
Fig. 11 Relationships between Charpy absorbed energy above DBTT and tensile properties ((a) ultimate tensile strength, (b) 0.2% proof stress, (c) uniform elongation, (d) total elongation, and (e) reduction in area) at the same test temperature for the as-received pure W and W-3%Re hot-rolled plates in the present study and the as-received pure W hot-rolled plate with a thickness of 4 mm [17]. Charpy absorbed energy is obtained by Charpy impact tests of KLST specimens (L-S direction). Tensile test is performed using SS-J specimens along L direction under strain rate of 1×10^{-3} s^{-1}.